PHYSICAL REVIEW B

CONDENSED MATTER

THIRD SERIES, VOLUME 35, NUMBER 4 1 FEBRUARY 1987

Nonlinear effects in quasielastic neutron scattering: Exact line-shape calculation for a dimer

V. M. Kenkre and G. P. Tsironis

Department of Physics and Astronomy, University of New Mexico, Albuquerque, New Mexico 87131

(Received 28 July 1986)

An exact solution of a discrete nonlinear Schrödinger equation, obtained recently for the site occupation probabilities in a two-site system such as a molecular dimer, has shown that the probabilities evolve in the form of Jacobian elliptic functions and exhibit a self-trapping transition. On the basis of that solution, we examine the effect of nonlinearities on the quasielastic scattering function in a dimer. The calculation is appropriate to the scattering of probe particles such as neutrons off moving quasiparticles which interact with lattice vibrations strongly enough to produce nonlinear effects while moving in the lattice. A well-known example is provided by hydrogen atoms diffusing among sites around impurities, e.g., oxygen, in metals such as niobium. Our calculation results in explicit expressions for the scattering spectrum. They exhibit the phenomenon of motional narrowing even in the absence of true damping. Comparison of the results for the undamped nonlinear dimer and the damped linear dimer uncover striking similarities as well as differences.

I. INTRODUCTION

The purpose of the analysis presented in this paper is to gain insights into the effects that nonlinearity in the evolution of quantum systems can have on experimentally observable quantities. The nonlinear evolution of interest is that typified by the discrete nonlinear Schrödinger equation[1-3]

$$\frac{dc_m(t)}{dt} = -i \sum_n V_{mn} c_n + i\chi \mid c_m \mid^2 c_m \tag{1.1}$$

and the specific observable studied is the quasielastic neutron scattering function $S(q,\omega)$.

An example of a physical system described by (1.1) is a quasiparticle, such as an exciton,[2] an electron,[3] or a light interstitial atom[4] (a hydrogen atom or an "isotope" such as a muon), moving among the sites of a crystal and interacting with the vibrations of the crystal. In (1.1), c_m is the amplitude for the system to be in state $\mid m \rangle$, V_{mn} is the intersite matrix element describing the transfer of the particle from state $\mid n \rangle$ to state $\mid m \rangle$, and χ is the nonlinearity parameter. The state $\mid m \rangle$ is the (localized) Wannier state centered on site m, V_{mn} directly gives rise to the bandwidth of the bare particle, and the nonlinearity parameter χ is the energy lowering due to polaronic effects. In the small-polaron literature[5-7] the quantity χ is often written as a sum of the products of the vibrational energies of the participating modes and the square of their coupling constants with the moving particle. The nonlinearity in the evolution inherent in (1.1) arises from the strong interaction of the moving quasiparticle with the vibrations of the crystal. There has been a resurgence of interest in this area.[8-12] Two types of questions are relevant: What is the particular kind (and strength) of interaction between the quasiparticle and the vibrations that will lead to (1.1) or similar nonlinear equations? And, what are the consequences of equations such as (1.1) for specific experimental observations? The first question addresses the validity of the assumptions made and procedures employed in the derivation of (1.1) for given Hamiltonians.[2,10,11] The second seeks to elucidate what effects, if any, would appear in observable quantities as a consequence of the nonlinearity.[12] In the present paper our interest lies solely in the second question.

The dynamics of particles such as light interstitial atoms, e.g., hydrogen atoms moving in a solid, is often studied with the help of the scattering of probe particles such as neutrons.[4,13-17] In such studies, attention is focused on the scattering function $S(q,\omega)$ which measures the extent of scattering of the probe particles with momentum transfer q and energy transfer ω ($\hbar=1$ throughout this paper). The scattering function $S(q,\omega)$ is connected to the self-correlation function $I(q,t)$ through the well-known van Hove relation[18,19]

$$S(q,\omega) = (1/2\pi) \int_{-\infty}^{+\infty} dt\, e^{-i\omega t} I(q,t) , \tag{1.2}$$

$$I(q,t) = (\mathrm{Tr} e^{-\beta H})^{-1} \mathrm{Tr} e^{-\beta H} e^{iqx} e^{itH} e^{-iqx} e^{-itH} . \tag{1.3}$$

At high temperatures, the self-correlation function $I(q,t)$

can be well approximated by the space-Fourier transform of the probability propagator, i.e., of the probability that the moving particle is at site m in the crystal at time t if it were at site 0 at the initial time.[16] We take the solid under consideration to be a crystal, and therefore, as a result of translational invariance, use only one index—m—to describe the propagator. This high-temperature connection between $I(q,t)$ and the probability propagator may be obtained trivially from (1.3) by taking the limit $\beta \to 0$ and therefore replacing $e^{-\beta H}$ by the identity operator.[16,20,21] The calculation of $S(q,\omega)$ for arbitrary temperatures can be carried out through an extension[16,21] of this high-temperature procedure.

The analysis in the present paper will be restricted to quasiparticles moving between the sites of a dimer, or of a collection of independent dimers. In the area of light interstitial transport,[4] an example is provided by trapped hydrogen atoms which move among sites in the neighborhood of impurity atoms such as those of oxygen placed in a metal, e.g., niobium.[14,15] The hydrogen atoms, more precisely protons, interact strongly with the lattice and are believed to exhibit polaronic effects.[22] Neutron scattering experiments[14,15] have probed this motion, have uncovered interesting line shapes, and have been interpreted in terms of a coexistence of tunneling and hopping of the protons among a small number of trapping sites. If, as is often done for simplicity, this number is taken to be effectively two, the system under investigation becomes a dimer.

For the dimer, q in the expression (1.2) for the scattering spectrum takes on two values,[23] 0 and π, and the corresponding space-Fourier components of the probabilities are, respectively, the sum and the difference of the two probability propagators for the dimer. The former equals 1 for all times—as a result of the conservation of probability—and has the trivial time-Fourier transform $S(0,\omega)=\delta(\omega)$. The nontrivial quantity which contains information about the evolution of the dimer is $S(\pi,\omega)$, and is given by

$$S(\omega) \equiv S(\pi,\omega) = (1/2\pi) \int_{-\infty}^{+\infty} dt\, e^{-i\omega t} p(t) , \tag{1.4}$$

where $p(t)$ is the difference of the two probability propagators. The observed $S(\mathbf{q},\omega)$ in an actual experiment is given by the weighted sum of $S(0,\omega)$ and $S(\pi,\omega)$

$$S(\mathbf{q},\omega) = \delta(\omega)\cos^2 q_1 + S(\omega)\sin^2 q_1 \tag{1.5}$$

where q_1 is the (dimensionless) projection of the momentum transfer vector $\mathbf{q}$ on a unit vector along the direction connecting the two sites in the dimer.[24] Henceforth in this paper, we shall be concerned only with the quantity $S(\omega)$.

As our interest lies in the dimer, we take m,n in (1.1) to assume values 1 and 2 only. Thus, (1.1) takes the form

$$i\frac{dc_1}{dt} = Vc_2 - \chi |c_1|^2 c_1 , \tag{1.6}$$

$$i\frac{dc_2}{dt} = Vc_1 - \chi |c_2|^2 c_2 . \tag{1.7}$$

The goal of the analysis in this paper is the calculation of the scattering function $S(\omega)$ as the time-Fourier transform of the probability difference $p(t) \equiv |c_1|^2 - |c_2|^2$. For the infinite-temperature case, the initial condition to be used in obtaining $p(t)$ is that of single-site occupation. The resulting expression for $S(\omega)$ is derived in Sec. II and the behavior of the scattering function for infinite temperature explored in some detail. Interesting similarities of these results for the nonlinear undamped dimer with those for a linear damped dimer are uncovered during this exploration. They are elaborated upon in Sec. III. The theory is extended for arbitrary temperatures in Sec. IV and a discussion is presented in Sec. V. Details of derivations are to be found in the Appendix.

II. SCATTERING FUNCTION FOR LARGE TEMPERATURES ($T \to \infty$)

The mathematical exercise at the heart of this paper consists of two steps: the calculation of $p(t)$ from (1.6) and (1.7), and the evaluation of its time-Fourier transform. A conversion of (1.6) and (1.7) to evolution equations for the density matrix, followed by an exact elimination of the density-matrix elements off-diagonal in the site representation, leads[12] to the following nonlinear equation for $p(t)$:

$$\frac{d^2p}{dt^2} = Ap - Bp^3 , \tag{2.1}$$

$$A = (\chi^2/2)p_0^2 - 4V^2 - 2V\chi(\rho_{21}+\rho_{12})_0, \quad B = (\chi^2/2) \tag{2.2}$$

where the subscript 0 denotes the initial value (at $t=0$). The general solution of (2.1) is given by[12]

$$p(t) = C\,\mathrm{cn}[(C\chi/2k)(t-t_0)\,|\,k] = C\,\mathrm{dn}[(C\chi/2)(t-t_0)\,|\,1/k] , \tag{2.3}$$

$$1/k^2 = 2 + (1/C^2)[(4V/\chi)^2 + (8V/\chi)(\rho_{21}+\rho_{12})_0 - 2p_0^2] , \tag{2.4}$$

where C and t_0 are arbitrary constants to be determined from the initial conditions, e.g., the values of p and dp/dt at $t=0$. Although the cn and dn (elliptic) functions in (2.3) are interrelated through the well-known Jacobi (real) reciprocal transformation,[25] normal usage represents the function as cn if $k \leq 1$ and as dn if $k \geq 1$. To avoid confusion we stress that, in this paper, we have used the symbol k to represent the elliptic parameter of the cn function, irrespective of whether $k \geq 1$ or $k \leq 1$. Details of the passage from (1.6) and (1.7) to (2.1) and (2.2), and of the evaluation of C and t_0 are in the Appendix.

Since, in this section, our interest lies only in the infinite-temperature result, we seek $p(t)$ for the condition that only one of the two sites is occupied initially. The quantities p_0 and $(dp/dt)_0$ are then, respectively, 1 and 0 with the consequence that, in (2.3) and (2.4), C equals 1 and t_0 equals 0. Equation (2.4) shows that k equals $\chi/4V$ for this initial condition, and the full solution of $p(t)$, which we require for the calculation of the scattering function, is given explicitly by

$$p(t) = \begin{cases} \mathrm{cn}\,(2Vt\,|\,\chi/4V) & \text{for } \chi < 4V , \quad (2.5a) \\ \mathrm{sech}(2Vt) = \mathrm{sech}(\frac{1}{2}\chi t) & \text{for } \chi = 4V , \quad (2.5b) \\ dn(\frac{1}{2}\chi t\,|\,4V/\chi) & \text{for } \chi > 4V . \quad (2.5c) \end{cases}$$

Detailed comments concerning the time behavior of the solutions (2.5) may be found elsewhere.[12] The time-Fourier transform of $p(t)$, required here for the calculation of the scattering function, can be written down immediately from (2.5) since each of the two Jacobian elliptic functions in (2.5) can be expressed explicitly as an infinite series of cosines.[26] Thus, for instance, the conjunction of (1.4) and (2.5a) leads to the scattering function

$$S(\omega)=\pi[kK(k)]^{-1}[Q^{n+1/2}(1+Q^{2n+1})^{-1}][\delta(\omega-\omega_n)+\delta(\omega+\omega_n)] \quad \text{for } \chi<4V\ , \tag{2.6}$$

valid for the "free" case, i.e., for $\chi<4V$. In (2.6), the frequencies ω_n are given by $[\pi V/K(k)][2n+1]$, the so-called nome Q equals $\exp[-\pi K(k')/K(k)]$, K is the complete elliptic integral of the first kind, $k=\chi/4V$, and $k'=(1-k^2)^{1/2}$. By dividing the summand in (2.6) by $Q^{n+1/2}$, the scattering function can be expressed as a sum of sech functions. Indeed, the three respective expressions for $S(\omega)$ corresponding to (2.5) are

$$S(\omega)=\begin{cases} \pi[2kK(k)]^{-1}\sum_{n=0}^{\infty}[\operatorname{sech}(\omega R_<)][\delta(\omega-\omega_n)+\delta(\omega+\omega_n)] & \text{for } \chi<4V\ , \quad (2.7a)\\ (1/4V)\operatorname{sech}(\omega\pi/4V)=(1/\chi)\operatorname{sech}(\omega\pi/\chi) & \text{for } \chi=4V\ , \quad (2.7b)\\ \pi[2K(1/k)]^{-1}\left[\delta(\omega)+\sum_{n=1}^{\infty}[\operatorname{sech}(\omega R_>)][\delta(\omega-\omega_n)+\delta(\omega+\omega_n)]\right] & \text{for } \chi>4V\ , \quad (2.7c)\end{cases}$$

where $R_<(k)$ equals $(1/2V)K(k')$, and $R_>(k)=(1/k)R_<(1/k)$. Both tend to $\pi/4V=\pi/\chi$ at the transition. It should be noted that k equals $\chi/4V$ on *both sides of the transition,* that the index n runs from 0 to ∞ in (2.7a) but from 1 to ∞ in (2.7c), and that the frequencies ω_n in (2.7a) are different from those in (2.7c). In (2.7a), i.e., on the free side of the transition, the ω_n are given by

$$\omega_n=(n+\tfrac{1}{2})[2\pi V/K(k)]=(n+\tfrac{1}{2})4V_{\text{eff}} \quad \text{for } \chi<4V\ , \tag{2.8}$$

where $n\geq 0$ as in the summation in (2.7a), and the quantity $V_{\text{eff}}\equiv[\pi V/2K(k)]$ is the effective intersite-matrix element[12] which describes the effective reduced bandwidth or velocity of the moving quasiparticle. On the other hand, in (2.7c), i.e., on the "self-trapped" side of the transition, the frequencies are given by

$$\omega_n=n[\pi\chi/2K(1/k)] \quad \text{for } \chi>4V\ , \tag{2.9}$$

with $n\geq 1$ as in the summation in (2.7c). Equations (2.7) constitute one of the central results of the present paper. The solutions (2.5) for the probability difference in the time domain correspond, in cases (2.5a), (2.5b), and (2.5c) to free motion, transition behavior, and self-trapped motion, respectively. The cn solution, i.e., case (2.5a) describes the oscillations of the moving quasiparticle, e.g., the hydrogen atom, between the two sites of the dimer in a manner similar to linear motion in a degenerate dimer. This behavior arises when the nonlinearity parameter is not too large, specifically when $\chi<4V$. As $\chi/4V$ increases in value, the nonlinearity increases in importance, the cn function departs increasingly from its trigonometric limit, i.e., $\cos(2Vt)$ (which it equals in the absence of the nonlinearity), and the quasiparticle moves more and more sluggishly between the two sites. At the transition, i.e., when $\chi=4V$, the quasiparticle takes infinite time to move between the two sites and $p(t)$ becomes identical to $\operatorname{sech}(2Vt)$. This is the case of (2.5b). Beyond the transition, as χ exceeds $4V$, $p(t)$ oscillates incompletely (i.e., the probability of the initially unoccupied site never reaches 1) as in the case of a linear nondegenerate dimer. Eventually, as $\chi/4V\rightarrow\infty$, $p(t)$ tends to the constant value 1 for all times and the quasiparticle never leaves the initially occupied site.

This interesting behavior of $p(t)$ is naturally reflected in the scattering function $S(\omega)$ as given by (2.7). In the free region ($\chi<4V$), symmetrically placed lines appear on the ω axis but there is no peak at $\omega=0$. In the self-trapped region ($\chi>4V$), however, an additional peak appears at $\omega=0$, corresponding to the fact that the average of $p(t)$ for this case does not vanish, in keeping with the effective energy mismatch which arises in this region as a result of the nonlinearity in the evolution. Figures 1 and 2 show the detailed evolution of $S(\omega)$ as the nonlinearity parameter is changed. In the absence of the nonlinearity, $k=0$ in (2.7). In this limit $K(k)$ tends to $\pi/2$ while $K(k')$ tends to infinity. Utilizing the limiting identity[25]

$$\lim_{k\rightarrow 0}(1/k)\{\exp[-\pi K(k')]/2K(k)\}=\tfrac{1}{4}\ ,$$

the spectrum of $S(\omega)$ is shown to consist of the two δ-function lines at $\pm 2V$ appropriate to a dimer with no nonlinearity. This is seen in Fig. 1(a). As the nonlinearity parameter χ becomes nonzero, an infinite number of δ-function lines appear throughout the ω region, specifically at $\omega_n=\pm(n+\frac{1}{2})(\Delta\omega)$, where $\Delta\omega$ is given by (for $\chi<4V$).

$$\Delta\omega=4V_{\text{eff}}=4V[(2/\pi)K(\chi/4V)]^{-1}\ . \tag{2.10}$$

As $\chi/4V$ increases, the intensity of the two original lines decreases whereas that of the new lines increases. All lines march towards the origin. No lines appear on the

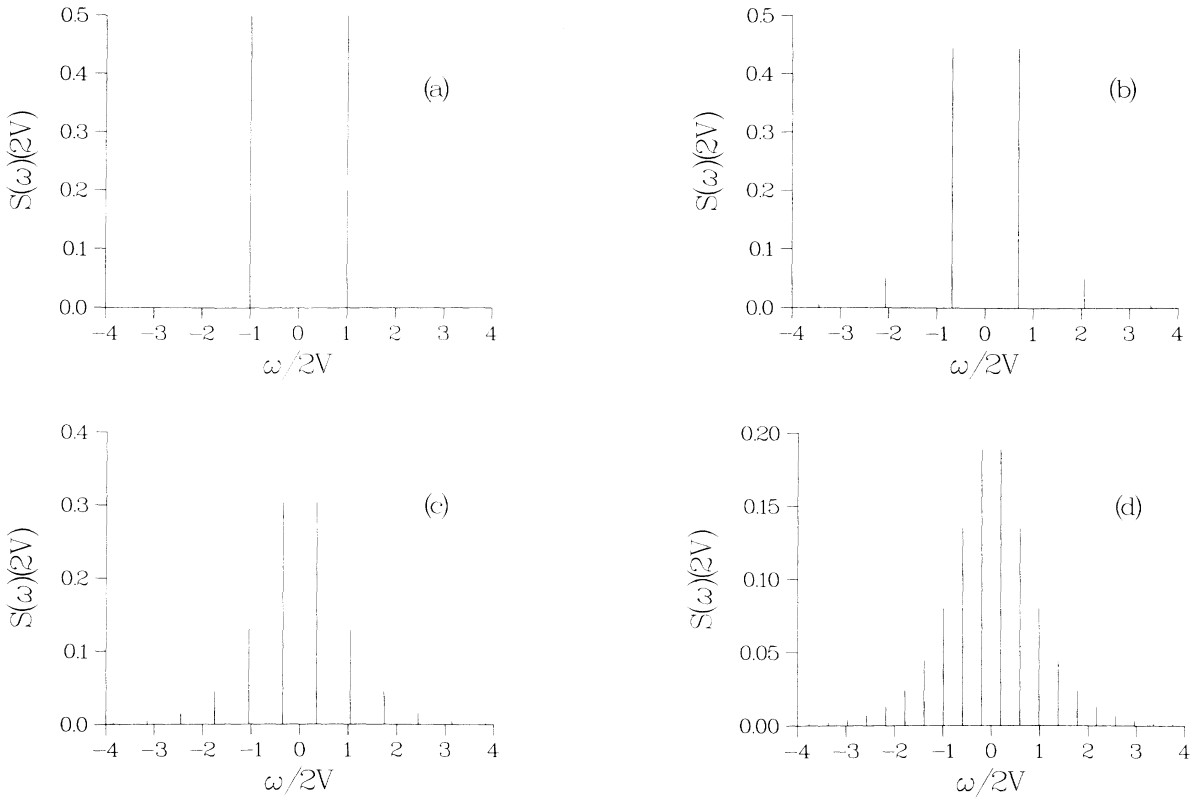

FIG. 1. Quasielastic neutron scattering line shape (scattering function) for a dimer, showing the effect of nonlinearity in the evolution in the free region ($\chi < 4V$) for several values of $\chi/4V$: (a) 0, (b) 0.9, (c) 0.999, (d) 0.999 999. As the nonlinearity increases, the lines are shifted towards the origin and the frequency interval $\Delta\omega$ decreases.

origin side of the original (largest intensity) lines. The frequency interval between any two neighboring lines in $\Delta\omega$. The decrease of $\Delta\omega$ and the march of the lines is seen clearly in Fig. 1 for successively higher values of $\chi/4V$.

When χ equals $4V$, the quasiparticle motion undergoes the free-to-self-trapped transition. The transition is reflected in $S(\omega)$ in a collapse of the δ functions onto a continuous finite scattering function, viz., $\mathrm{sech}(\pi\omega)$, as given by (2.7b). Figure 2(a) shows this transition case. It is interesting to compare (2.5b) and (2.7b) and note here that, like the Gaussian, the sech function is invariant under a Fourier transform.

As the nonlinearity increases beyond the transition value, i.e., as $\chi > 4V$, the continuous finite scattering function $\mathrm{sech}(\pi\omega)$ breaks up into a infinite number of δ-function lines again. A line appears at $\omega = 0$ and it grows as the nonlinearity parameter increases. It represents the effective energy mismatch arising from the nonlinearity in the evolution. The other lines march outwards away from the origin and decrease in intensity as $\chi/4V$ increases. This fascinating behavior of $S(\omega)$, which is shown explicitly by (2.7c) and Figs. 2(b)—(d), is nothing other than *motional narrowing* which is well known in the case of the scattering spectrum for a linear damped system.

The frequency interval $\Delta\omega$ is given by (2.10) for $\chi < 4V$, but by

$$\Delta\omega = \chi[(2/\pi)K(4V/\chi)]^{-1} \tag{2.11}$$

for $\chi > 4V$. In Fig. 3, we show its variation for all values of $\chi/4V$. At the transition, $\Delta\omega$ equals zero and marks the collapse of the δ functions of $S(\omega)$ onto the finite function as given by (2.7b). On both sides of the transition, $\Delta\omega$ rises as shown, its limiting value being $4V$ in the free region and χ, therefore infinite, in the self-trapped region. A good approximation to its value in the neighborhood of the transition is given by

$$\Delta\omega \approx \begin{cases} 4V\pi/\ln\{16[1-(\chi/4V)^2]^{-1}\} & \text{for } \chi \lesssim 4V \quad (2.12) \\ \chi\pi/\ln\{16[1-(4V/\chi)^2]^{-1}\} & \text{for } \chi \gtrsim 4V\,. \quad (2.13) \end{cases}$$

The results of this section are valid for temperatures T large enough, i.e., $\beta = (1/k_B T)$ small enough, to allow the replacement of $e^{-\beta H}$ by the identity operator. In an approximate sense this requirement may be expressed as $V \lesssim k_B T$, i.e., that the bandwidth be small with respect to the thermal energy.

III. COMPARISON WITH RESULTS FOR THE LINEAR DIMER

We have seen in Sec. II that the scattering spectrum for the *nonlinear undamped* dimer, as given by (2.7) and

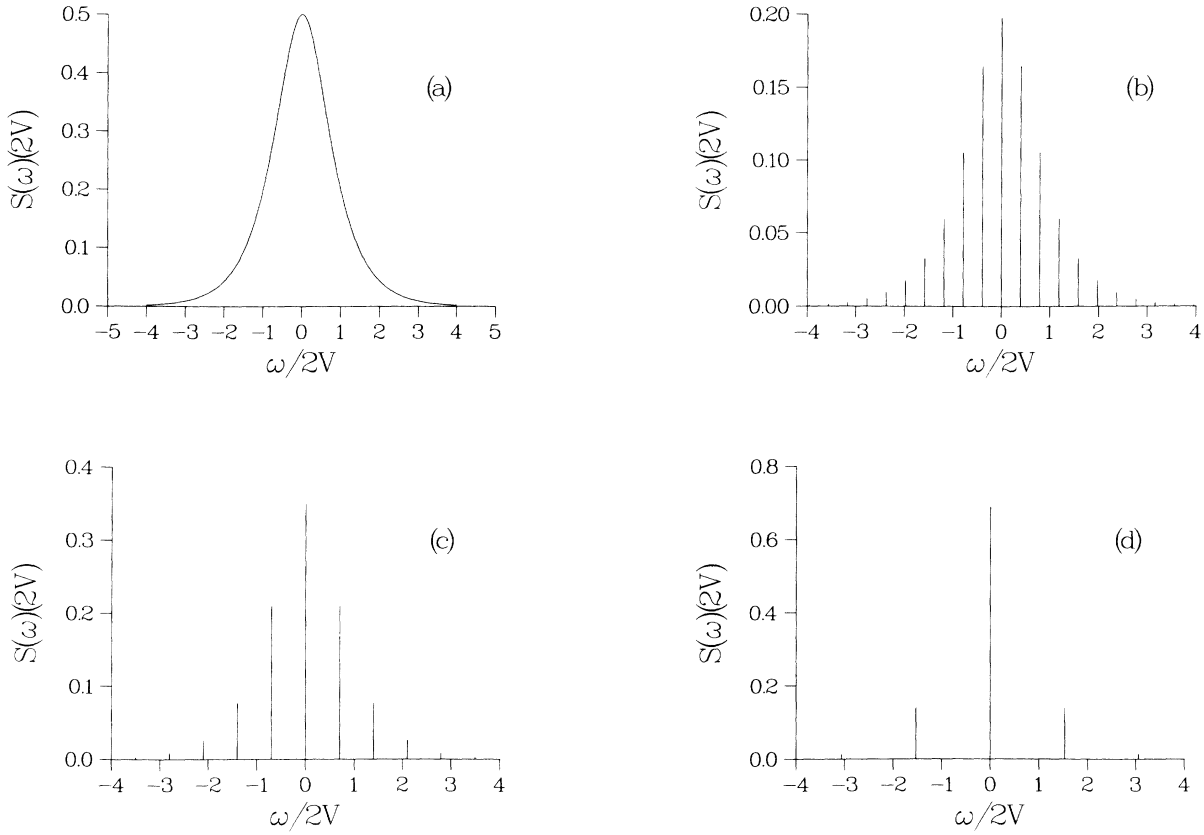

FIG. 2. Scattering function showing the effect of nonlinearity in the evolution in the transition and self-trapped regions ($\chi \geq 4V$) for several values of $4V/\chi$: (a) 1, (b) 0.999 999, (c) 0.999, (d) 0.9. The δ functions collapse onto a finite curve in the transition case (a). As the nonlinearity increases beyond the transition, the δ functions return, the central line grows, the other lines march outwards from the origin, and the frequency interval $\Delta\omega$ increases to infinity.

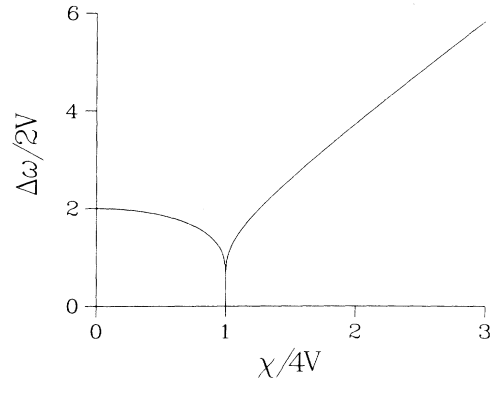

FIG. 3. The frequency interval $\Delta\omega$ between lines in the scattering spectrum of the nonlinear dimer as a function of the nonlinearity parameter $\chi/4V$. An increase in the latter results in a decrease (increase) in $\Delta\omega$ in the free (self-trapped) region. At the transition, $\Delta\omega$ equals to zero.

shown in Figs. 1 and 2, possesses an envelope that exhibits the phenomenon of broadening in the free region and that of motional narrowing in the self-trapped region. This behavior is strikingly similar to that obtained in a *linear damped* dimer as a comparison of Figs. 1 and 2 with Fig. 4 below will show. We explore these similarities and investigate the differences for these two systems in this section.

The evolution equation for a particle moving between the sites of a linear damped dimer is expressed conveniently in the form of the stochastic Liouville equation[16,27–29] (SLE) for the density-matrix elements. The equation for ρ_{11} is identical to (A1) but that for ρ_{12} is different:

$$d\rho_{12}/dt = -iV(\rho_{22}-\rho_{11})-\alpha\rho_{12} \ . \tag{3.1}$$

Corresponding equations describe the evolution of the other two elements. The parameter α is the rate of damping or of scattering of the "Bloch" states of the dimer. The equation obeyed by the probability difference $p(t)$ is the same as that obeyed by the damped harmonic oscillator with suitable correspondences:

$$\frac{d^2p}{dt^2}+\alpha\left[\frac{dp}{dt}\right]+4V^2p=0 \tag{3.2}$$

and results[30] in the following well-known solution for $p(t)$:

$$p(t)=\begin{cases} e^{-t\alpha/2}[\cos(\Omega_< t)+(\alpha/2\Omega_<)\sin(\Omega_< t)] & \text{for } \alpha<4V\,, \quad (3.3a)\\ e^{-t\alpha/2}[1+(t\alpha/2)]=e^{-2Vt}[1+2Vt] & \text{for } \alpha=4V\,, \quad (3.3b)\\ e^{-t\alpha/2}[\cosh(\Omega_> t)+(\alpha/2\Omega_>)\sinh(\Omega_> t)] & \text{for } \alpha>4V\,. \quad (3.3c)\end{cases}$$

Here $\Omega_<$ is given by $[4V^2-(\alpha/2)]^{1/2}$, and $\Omega_>$ by $[(\alpha/2)^2-4V^2]^{1/2}$. Equations (3.3) for the linear damped dimer should be compared to (2.5) which describe the nonlinear undamped dimer.

The time-Fourier transform of (3.3) is trivial to calculate. The resulting scattering spectrum is given by

$$S(\omega)=\begin{cases} [2+(\omega/\Omega_<)]\mathscr{L}_\alpha(\omega+\Omega_<)+[2-(\omega/\Omega_<)]\mathscr{L}_\alpha(\omega-\Omega_<) & \text{for } \alpha<4V\,, \quad (3.4a)\\ 2\{1+\cos[2\tan^{-1}(2\omega/\alpha)]\}\mathscr{L}_\alpha(\omega) & \text{for } \alpha=4V\,, \quad (3.4b)\\ [\mathscr{L}_+(\omega)+(\alpha/2\Omega_>)\mathscr{L}_-(\omega)] & \text{for } \alpha>4V\,, \quad (3.4c)\end{cases}$$

where $\mathscr{L}_\alpha(\omega)$ is $(1/2\pi)$ times the Lorentzian $(\alpha/2)[(\alpha/2)^2+\omega^2]^{-1}$, and $\mathscr{L}_\pm(\omega)$ equals $\mathscr{L}_{\alpha-2\Omega}(\omega)\pm\mathscr{L}_{\alpha+2\Omega}(\omega)$. We have chosen to display the spectrum expressions in the form (3.4) rather than in the more commonly encountered simple form

$$\pi S(\omega)=(4V^2\alpha)[(4V^2-\omega^2)^2+(\omega\alpha)^2]^{-1} \quad (3.5)$$

to facilitate their comparison with the nonlinear expressions (2.7). The spectrum $S(\omega)$ is shown in Fig. 4 for various values of $\alpha/4V$. The spectrum starts out in the absence of damping ($\alpha=0$) as the two δ functions as in Fig. 1(a). However, the damping inherent in α brings about a true broadening of the spectrum rather than a splitting of the two original lines into an infinity of lines as observed for the nonlinear undamped case. An increase in the damping parameter $\alpha/4V$ leads both to an increase in the broadening of the two peaks and to a shift of the peaks towards the origin. When $\alpha=4V$, the two peaks coalesce into a single peak at the origin. In the language of the damped harmonic oscillator, one has *critical* damping. As $\alpha/4V$ increases further, the central peak is seen to grow, turning into a δ function at the origin for $\alpha/4V\to\infty$.

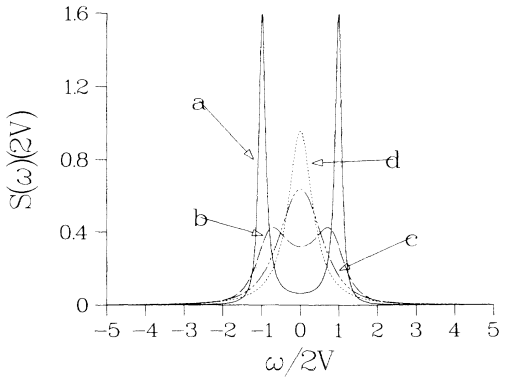

FIG. 4. Scattering function for a *linear damped* dimer, showing the effect of damping for several values of $\alpha/4V$: (a) 0.1, (b) 0.5, (c) 1, (d) 1.5. The familiar phenomena of broadening and motional narrowing are evident.

The comparison of the linear damped case with the nonlinear undamped case is straightforward. The transition situation $\chi=4V$ in the latter corresponds to critical damping $\alpha=4V$ in the former. Both represent infinitely sluggish equalization of site probability on the two sites and result in a finite line shape for the scattering spectrum. When the damping parameter α (correspondingly the nonlinearity parameter χ) is smaller than $4V$, the line-shape peaks march towards the origin with increasing $\alpha/4V$ (correspondingly $\chi/4V$). The peaks are finite in the linear damped case but δ functions in the nonlinear undamped case. The frequency interval between the peaks, viz., $\Delta\omega$, is given by $4V_{\text{eff}}$ in the latter case and may be approximated by $2\Omega_<$ in the former. Figure 5(a) shows that the variation of $\Delta\omega$ in the "underdamped (free)" region is quite similar in the two cases. Equation (2.7c) shows that, with increasing $\chi/4V$ in the self-trapped region, the line at $\omega=0$ grows at the expense of the rest of the spectrum. Equation (3.4c) shows similarly that, with increasing $\alpha/4V$ in the "overdamped" region, the peak at $\omega=0$ grows at the expense of the rest of the spectrum. In the nonlinear case, the intensity of the growing part of the spectrum, relative to that of the entire spectrum, is given by $\pi/[2K(4V/\chi)]$, the coefficient of $\delta(\omega)$. Although it is more difficult to select an appropriate quantity to describe the relative growth of the central peak in the linear case because of the absence of δ functions, we take it to be $2\Omega_>/\alpha$, the ratio of the value of $[\mathscr{L}_-(\omega)]_{\omega=0}$ to that of $[\mathscr{L}_+(\omega)]_{\omega=0}$. Figure 5(b) shows that the variation of the relative intensity of the growing part of the spectrum at $\omega=0$, defined in this manner, is also quite similar in the linear and nonlinear cases.

The source of this impressive similarity can be traced to

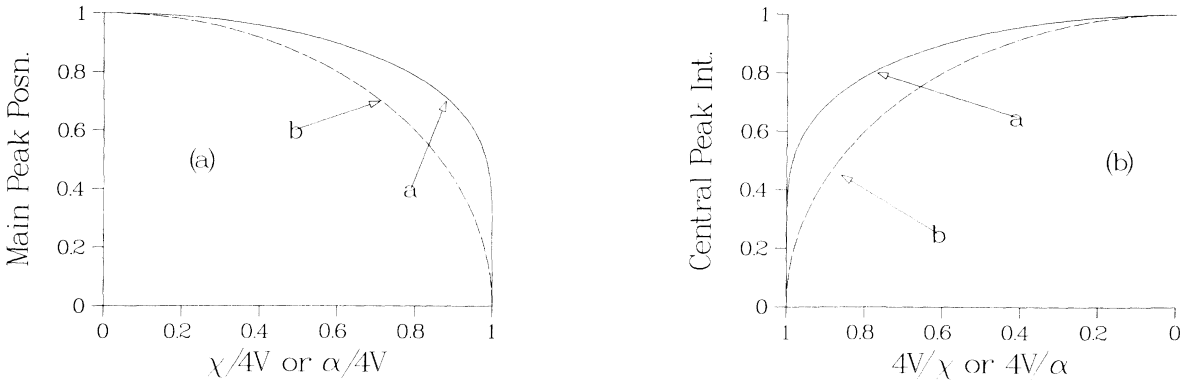

FIG. 5. Comparison of spectral features of the nonlinear undamped and the linear damped dimers showing similarities. In (a) the position of the main (largest) peak in the "free/underdamped" region is plotted as a function of a, the nonlinearity parameter $\chi/4V$ for the nonlinear dimer, and of b, the damping parameter $\alpha/4V$ for the linear dimer. In (b), the relative intensity of the central peak (see text) is plotted as a function of a, $\chi/4V$ and b, $\alpha/4V$. The behavior is similar in the two cases for both (a) and (b).

the fact that, if the nonlinearity parameter χ in the original amplitude equations (1.6), (1.7) for the *nonlinear undamped* dimer is taken to be imaginary (e.g., $\chi=i\alpha$ with α real), the off-diagonal part of the resulting density-matrix equation is identical to that of the stochastic Liouville equation (3.1) for the *linear damped* dimer. Thus, although the nonlinear equation (2.1) and the linear damped equation (3.2) for the probability difference $p(t)$ have completely different appearances and solutions, they both arise from (1.6), (1.7). If χ is purely real, (2.1) and nonlinear undamped dynamics results, whereas, if χ is purely imaginary, (3.2) and linear damped dynamics is the outcome. If χ is taken to be generally complex, a nonlinear integro-differential equation can be derived, the real part of χ being the nonlinear parameter and the imaginary part the damping parameter. That equation, which leads to a scattering spectrum which interpolates between that shown in Fig. 1 and that in Fig. 4, will be discussed elsewhere. Needless to say, whenever one uses a χ which is not purely real, the diagonal part of the ρ equation must be left untouched (in the same spirit as in the construction of the standard SLE) to ensure that the total particle probability does not decay.

The major difference between the scattering spectrum for the nonlinear undamped and the linear damped dimer is thus, that (with the exception of the "transition/critical" case) the line shape of δ functions in the former but is finite in the latter. Although no δ-function lines exist in a real system, the difference between the two spectra would be discernible experimentally, at least in principle, if the following three requirements are met: (i) The instrument broadening width should be small enough, (ii) the frequency interval $\Delta\omega$ [see (2.10), (2.11)] should be large enough, and (iii) the neighboring peaks should not be disparate in intensity. The spectrum for the nonlinear dimer will then consist of a multitude of peaks while that for the linear dimer will have at most two peaks. Requirement (i) refers to the quality of instrumentation and the extent to which the lines are free of extraneous interferences. Given a specific instrument broadening width, requirement (iii) places a window on the value of $\chi/4V(\alpha/4V)$ for which the difference in the two spectra is easily discernible. In Fig. 6(a) we show explicitly the difference that could arise in an experimentally determined spectrum depending on whether the interaction with the lattice results in damping as in (3.2) or in nonlinear evolution as in (2.1). Peak multiplicity is a clear signature of nonlinearity in this context. For contrast, we show Fig. 6(b) in which no direct clue appears in the shape of the spectrum which would allow one to distinguish between damping and nonlinearity. The values of the damping ratio $\alpha/4V$ and the nonlinearity ratio $\chi/4V$ have been taken to be identical to each other in Fig. 6(a) (0.95) and Fig. 6(b) (0.1), and the extent of instrument broadening, i.e., the width of the Lorentzian with which all line shapes in Fig. 6 have been convoluted, has been taken to be 0.05 (in units of $4V$).

Another obvious difference between the spectra for the linear damped and the nonlinear undamped dimer is in the spectral moments $\mathcal{M}_n$, which are defined as $\int_{-\infty}^{\infty} d\omega\,\omega^n S(\omega)$. For the nonlinear dimer, we can calculate the even moments directly from the evolution equation (2.1) with the help of the relation

$$\mathcal{M}_{2n}=(-1)^n[d^{2n}p(t)/dt^{2n}]_{t=0}\,.$$

The second and fourth moments are found to be $4V^2$ and $4V^2(4V^2+\chi^2)$, respectively. For the linear damped dimer, the second moment is $4V^2$ as in the nonlinear case; however, the fourth and higher moments all blow up as a result of the well-known breakdown of the damping model for short times, equivalently high frequencies. The odd derivatives of $p(t)$, as given by (3.2), are equal in magnitude but opposite in sign when evaluated on the two sides of $t=0$. Thus $(dp/dt)_0=0$ but $(d^3p/dt^3)_0=\pm 4V^2\alpha$. It follows from this multivalued nature of $(d^3p/dt^3)_0$ that the fourth moment of the spectrum for the linear damped dimer is infinite. This is also seen from (3.5). The damping model of (3.2) cannot be taken seriously for large ω in $S(\omega)$ or for large n in $\mathcal{M}_n$. On the other hand, our expressions (2.7) for the nonlinear dimer do not suffer from these shortcomings and can indeed be

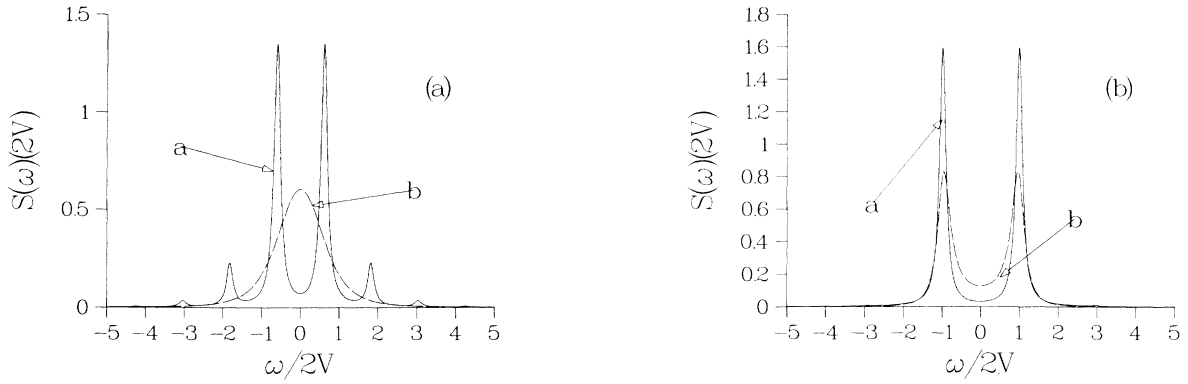

FIG. 6. Comparison of spectral features of the nonlinear undamped and the linear damped dimers showing differences. Both spectra are convoluted with a Lorentzian of width 0.05 (in units of $4V$), representing instrumental broadening as would appear in experimental observations. Values of the system parameter [$\chi/4V$ for curves a and $\alpha/4V$ for curves b] are (a) 0.95, and (b) 0.1. (a) shows the clear manifestation of nonlinearity in the multiplicity of peaks and illustrates a possible manner of distinguishing experimentally between the effects of nonlinearity and of damping. (b) shows how the difference could be masked in observed spectra.

used through moment expressions to extract the value of the nonlinearity from observed spectra.

IV. SCATTERING FUNCTION FOR ARBITRARY TEMPERATURES

Our analysis of the scattering function has been restricted so far to the case of infinite temperatures. This has been done for the specific purpose of showing the new effects of nonlinearity on the scattering observables without bringing in distractions that further aspects, such as finite temperatures, would introduce. We return to the case of finite temperatures in this section.

To analyze $S(\omega)$ for $T\neq\infty$, it is necessary to return to (1.3). By cyclic permutation of the operators in the trace in (1.3), one may write $I(q,t)$ as

$$I(q,t)=\mathrm{Tr}e^{-iqx}e^{-itH}M_{+}e^{itH} \tag{4.1}$$

where $M_{+}=(\mathrm{Tr}e^{-\beta H})^{-1}e^{-\beta H}e^{iqx}$. It follows that $I(-q,-t)$ is given by

$$I(-q,-t)=\mathrm{Tr}e^{-iqx}e^{-itH}M_{-}e^{itH} \tag{4.2}$$

where $M_{-}=(\mathrm{Tr}e^{-\beta H})^{-1}e^{iqx}e^{-\beta H}$. Straightforward manipulations from the general form of the response function lead[19] to the well-known result that, irrespective of the particulars of the system under analysis, $S(q,\omega)$ and $S(-q,-\omega)$ are interrelated through the detailed balance relation

$$S(q,\omega)=e^{\beta\omega}S(-q,-\omega)\ . \tag{4.3}$$

The prescription (1.2), (1.3) for the calculation of the scattering spectrum $S(q,\omega)$ is therefore exactly equivalent to the alternate prescription

$$S(q,\omega)=[e^{\beta\omega/2}\mathrm{sech}(\beta\omega/2)]\times(1/2\pi)\int_{-\infty}^{+\infty}dt\,e^{-i\omega t}I_S(q,t)\ , \tag{4.4}$$

$$I_s(q,t)=\mathrm{Tr}e^{-iqx}e^{-itH}Me^{itH}\ , \tag{4.5}$$

$$M=\tfrac{1}{2}(M_{+}+M_{-})=\tfrac{1}{2}(\mathrm{Tr}e^{-\beta H})^{-1}(e^{-\beta H}e^{iqx}+e^{iqx}e^{-\beta H})\ . \tag{4.6}$$

The infinite-temperature limit of (1.2) and (1.3), which we used in Sec. II, has the convenient feature that the scattering spectrum is given as the time-Fourier transform of the space-Fourier transform of the probability of site occupation. The advantage of the new prescription (4.4)—(4.6) over the straightforward use of (1.2) and (1.3) is that this convenient feature is retained for *arbitrary temperatures*. However, the probability whose double transform is the scattering spectrum, is to be calculated for a special initial condition[16] dictated generally by the temperature. The special initial "density matrix" is M, with M given by (4.6). This manipulation of the general response function which makes the arbitrary temperature prescription practically identical to the infinite temperature prescription was given and used earlier in the analysis of frequency-dependent mobilities[21] and also of the scattering function on a linear chain.[16]

The program of calculation to be followed for arbitrary temperatures is thus to obtain $p(t)$ (which, as explained in Sec. I, is the only nontrivial component of the space-Fourier transform in the case of a dimer) by solving its nonlinear evolution equation (2.1) not for the initial condition of occupation of a single site as in Sec. II, but for the initial density matrix, M, and then to evaluate the time-Fourier transform of $p(t)$. The value of q to be used in (4.6) is, as before, π. Taking the matrix elements of the position operator to be given by $\langle 1|x|1\rangle=0$, $\langle 2|x|2\rangle=1$, $\langle 1|x|2\rangle=\langle 2|x|1\rangle=0$, the matrix $e^{i\pi x}$ is written explicitly as

$$e^{i\pi x}=\begin{bmatrix}1 & 0\\ 0 & -1\end{bmatrix}\ . \tag{4.7}$$

The elements of M therefore satisfy

$$M_{11}-M_{22}=1\ , \tag{4.8}$$

$$M_{12}-M_{21}=0=M_{12}+M_{21}\ , \tag{4.9}$$

independently of the temperature detail contained in the elements of $e^{-\beta H}$. The remarkable result is therefore that $S(\omega)$ is given simply by

$$[S(\omega)]_T=[S(\omega)]_{T=\infty}[e^{\beta\omega/2}\mathrm{sech}(\beta\omega/2)]\ . \tag{4.10}$$

We conclude that the scattering spectrum for arbitrary temperatures can be obtained directly from the infinite-temperature result arrived at in Sec. II by simply multiplying it by the detailed balance factor. The resulting explicit expressions constitute an exact calculation of the scattering spectrum of a nonlinear dimer for arbitrary temperatures. We rewrite them here in a modified form:

$$S(\omega)=\begin{cases} B_{<}\sum_{n=0}^{\infty}[\delta(\omega-\omega_n)e^{\beta\omega_n/2}+\delta(\omega+\omega_n)e^{-\beta\omega_n/2}]\ , & \text{(4.11a)}\\ (1/2V)e^{\beta\omega/2}\{\cosh[(\omega/2)(\beta+\pi/2V)]+\cosh[(\omega/2)(\beta-\pi/2V)]\}^{-1}\ , & \text{(4.11b)}\\ \pi[2K(1/k)]^{-1}\delta(\omega)+B_{>}\sum_{n=1}^{\infty}[\delta(\omega-\omega_n)e^{\beta\omega_n/2}+\delta(\omega+\omega_n)e^{-\beta\omega_n/2}]\ . & \text{(4.11c)}\end{cases}$$

As in (2.7), the three cases (4.11a), (4.11b), and (4.11c) refer to $\chi<4V$, $\chi=4V$, and $\chi>4V$, respectively. The symbols $B_{<}$ and $B_{>}$ are given by

$$B_{<}=\pi[kK(k)]^{-1}\{\cosh[(\omega/2)(\beta+2R_{<})]+\cosh[(\omega/2)(\beta-2R_{<})]\}^{-1}\ , \tag{4.12}$$

$$B_{>}=\pi[K(1/k)]^{-1}\{\cosh[(\omega/2)(\beta+2R_{>})]+\cosh[(\omega/2)(\beta-2R_{>})]\}^{-1}\ . \tag{4.13}$$

Illustrative plots of the scattering spectrum for noninfinite temperatures are shown in Fig. 7.

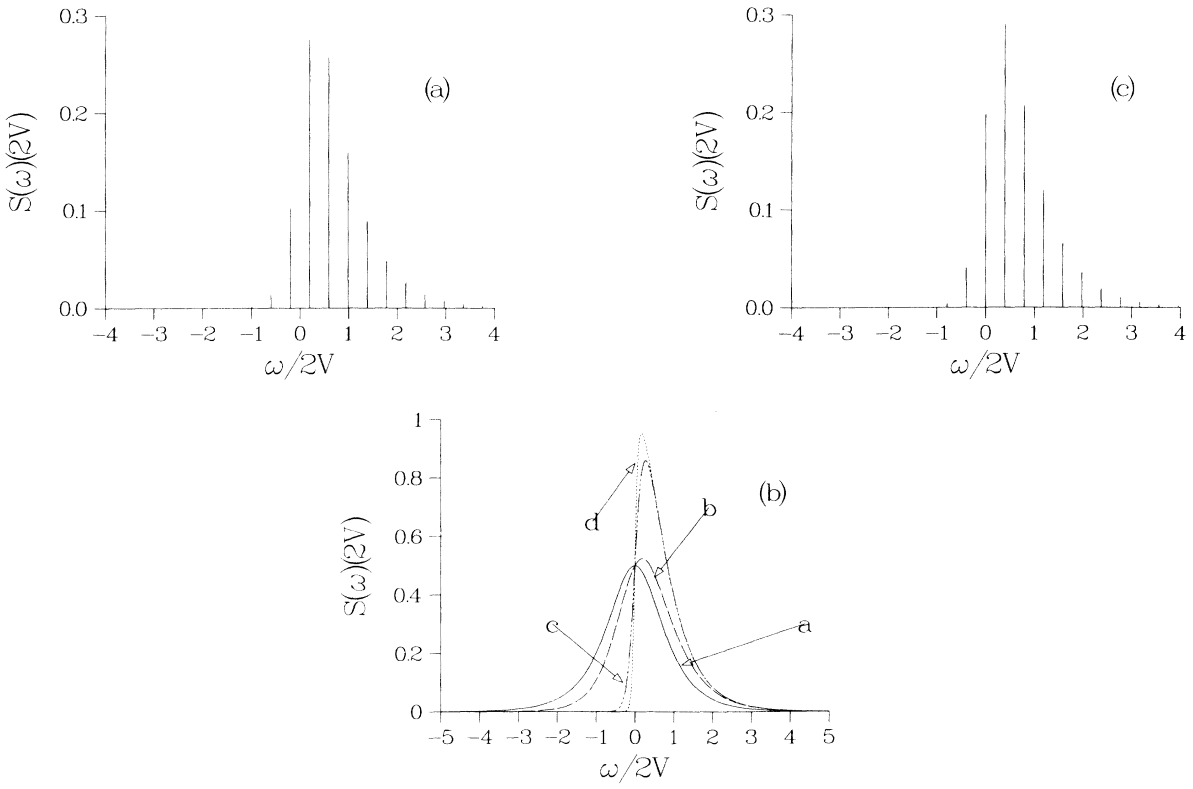

FIG. 7. Scattering function for the nonlinear dimer for arbitrary temperatures. In (a) and (c), the spectrum is shown for $k_BT/2V=0.2$ in the free region ($\chi/4V=0.999\,999$) and the self-trapped region ($4V/\alpha=0.999\,999$), respectively. The skewness of the spectrum arising from detailed balance is evident. In (b), which shows the spectrum for the transition region ($\chi=4V$), the dependence of the spectrum on temperature is seen clearly as the skewness increases with a decrease in temperature. The value of $k_BT/2V$ is for curve *a*, ∞; for curve *b*, 1; for curve *c*, 0.1; for curve *d*, 0.04.

V. DISCUSSION

The discrete nonlinear Schrödinger equation (1.1) appears to provide a powerful alternative to more traditional starting points in the study of quasiparticles interacting strongly with the lattice. Although its range of applicability and precise connection to microscopic details continue to be debated,[2,10,11] the richness of the physics it contains suggests strongly that it is important to explore its consequences in specific *observable quantities*. The present paper is the result of such an exploration in the particular context of the scattering function in a dimer.

Our calculation has the advantage that it involves no approximation procedures. However, it is directly applicable to a rather small system, viz., a dimer. The results of our analysis should find two uses: in the qualitative understanding of the effects of nonlinearity in extended systems, and in the quantitative interpretation of observations carried out specifically on systems of noninteracting dimers. Hydrogen atoms moving among trapping sites around impurities in metals[14,15] constitute only one of the examples for which our analysis is applicable. Others are excited dimers in aromatic hydrocarbon crystals such as 1,2,4,5-tetrachlorobenzene[31] studied with microwave probes via optically detected magnetic resonance, and "stick-dimers"[32] consisting of poly-L-proline oligamers of controllable length studied via measurements of fluorescence depolarization.[33]

The point of departure of our analysis is (1.6) and (1.7). Our final results are Eqs. (2.7) for infinite temperature and the generalization (4.11) for arbitrary temperature. Our primary findings are that the scattering spectrum for the nonlinear dimer exhibits motional narrowing as well as broadening in its envelope as seen in Figs. 1 and 2, and that, for appropriate parameter values, it consists of a multiplicity of peaks. The first of these findings shows similarity in behavior to the linear damped dimer whereas the second shows a marked difference. A comparison of Figs. 1 and 2 with Fig. 4 stresses the similarity, as do Figs. 5 and 6(b). On the other hand, the difference is shown in Fig. 6(a). Our motivation for carrying out the comparative analysis of the linear damped and the nonlinear undamped dimer arises from the fact that strong interaction with the lattice can give rise to nonlinearities as well as damping in the evolution of the quasiparticle. In view of the substantial apparent difference in the form of the equations obeyed by the probability difference $p(t)$ in the two cases [Eqs. (2.1) and (3.2), respectively], it is remarkable that the spectra possess profound similarities. Also of interest is the fact that those dissimilar equations arise from the same amplitude equations (1.6) and (1.7) when χ is purely real in one case and purely imaginary in the other. We believe that it will be fruitful to view microscopic interaction of the quasiparticle with the lattice in analogy with electromagnetic interaction of charges with matter. Just as detailed charge-matter interactions are reformulated in terms of a complex "dielectric constant" whose real (imaginary) part describes propagation (attenuation), detailed lattice-quasiparticle interactions might be reexpressed in terms of some complex "medium constant" whose real part χ (imaginary part α) would be responsible for nonlinearities (damping) in the evolution of the quasiparticle.

What are the experimental manifestations of the nonlinearity inherent in (1.1) which would not be present in an appropriate linear counterpart? This question is answered by Fig. 6(a). Peak multiplicity is the consequence of nonlinearity. The frequency interval between those peaks is *not* some vibration frequency as would be the case, e.g., in the optical spectrum of an impurity whose electronic excitation interacts strongly with vibrations.[34] The frequency interval is given by (2.10) or (2.11). It is proportional to an effective value of the bandwidth in the free region and of an energy mismatch in the self-trapped region. The absence of any striking difference in shape in the two spectra in Fig. 6(b) points to the possibility that observations which have been interpreted in the past in terms of a linear damping interaction could actually be stemming from a nonlinear interaction with little damping. Both χ and α contain in them information concerning the interaction with the lattice. It is not inconceivable, therefore, that appreciable revision in the values of quasiparticle-lattice coupling constants might be the outcome of a reinterpretation of scattering spectra.

The generalization of the infinite-temperature result (2.7) to (4.11), which is valid for arbitrary temperatures, requires comment. The prescription of Refs. 16 and 21, which has made that generalization possible, would be normally sensitive to the temperature detail present in M, the special initial density matrix of (4.6). However, it is a happy accident that the detail becomes irrelevant *for a dimer*. Although the elements of M do contain temperature information, the difference of the diagonal elements of M (in the site representation) equals 1 and is therefore independent of temperature. Furthermore, the off-diagonal elements of M are zero. The initial density matrix is thus formally "localized on a single site." The calculation of the symmetrized scattering function is then formally identical to that for infinite temperature and does not require additional information that would be present in the general solution (2.3) beyond (2.5).

If the simplification referred to above had not been operative in the dimer, a more complex analysis from (2.3) would have been necessary. Among the quantities that would have been required in that analysis are the coefficients in an expansion of the stationary states of the nonlinear dimer in terms of the site states. We mention in passing how these may be obtained from (2.3) and (2.4). When the system is in a stationary state, all elements of its density matrix, and consequently dp/dt as well as p [see (A3)—(A5)], are time independent. Equating d^2p/dt^2 to zero in (2.1) leads to $p=0$ or $p=(A/B)^{1/2}$. The former value of p corresponds to the usual delocalized stationary state with equal coefficients for both sites but the latter values represents a self-trapped state with unequal site occupation probabilities. When substituted in (2.2), $p^2=p_0^2=A/B$ yields

$$(4V/\chi)+2(\rho_{21}+\rho_{12})_0=0 \ . \tag{5.1}$$

Reexpressing the density-matrix elements in (5.1) in terms of the amplitudes c_1 and c_2, one arrives at

$$|c_1| = (1/2)^{1/2}\{1+[1-(2V/\chi)^2]^{1/2}\}^{1/2}, \quad (5.2)$$

$$|c_2| = (1/2)^{1/2}\{1-[1-(2V/\chi)^2]^{1/2}\}^{1/2}. \quad (5.3)$$

Equations (5.2) and (5.3) are clearly representative of an effective energy mismatch and agree with results obtained earlier[8] for the stationary state coefficients.

The system under analysis in this paper could appear at first sight to be too trivial to deserve attention because it consists merely of two sites. However, the importance of understanding the physics of dimers has been amply realized in various different contexts. For instance, considerable effort has been devoted to the study of two-state systems in the field of energy transfer in molecular solids, on the experimental[31,32,35–37] as well as the theoretical front.[33,37–41] The motivation for that effort, as well as that for our own analysis here, comes both from the direct applicability of the dimer results to experiments, and from the insights that dimers can provide for the understanding of more complex extended systems. Along the latter lines we hope that the results reported in this paper will be of use to general investigations concerning the statistical mechanics of solitons in extended systems.[42,43]

ACKNOWLEDGMENTS

It is a pleasure for us to thank David Campbell and Daniel Finley for helpful conversations, and David Dunlap and Rebecca Dicks for advice concerning numerical computations. This work was supported in part by the National Science Foundation under Grant No. DMR-85-06438.

APPENDIX

1. Derivation of the nonlinear equation (2.1) from (1.6) and (1.7)

In terms of the density-matrix elements $\rho_{11}=c_1^* c_1$, $\rho_{12}=c_1^* c_2$, etc., Eqs. (1.6) and (1.7) are rewritten as

$$d\rho_{11}/dt = -iV(\rho_{21}-\rho_{12}), \quad (A1)$$

$$d\rho_{12}/dt = -iV(\rho_{22}-\rho_{11})+i\chi(\rho_{11}-\rho_{22})\rho_{12}, \quad (A2)$$

with corresponding equations for ρ_{22} and ρ_{21}. They lead to the following coupled equations for the probability difference $p(t)\equiv\rho_{11}-\rho_{22}$, the difference $\rho_{21}-\rho_{12}$ of the off-diagonal elements of ρ, and their sum $\rho_{21}+\rho_{12}$:

$$\frac{dp}{dt} = -i2V(\rho_{21}-\rho_{12}), \quad (A3)$$

$$\frac{d(\rho_{21}-\rho_{12})}{dt} = -i2Vp - i\chi p(\rho_{21}+\rho_{12}), \quad (A4)$$

$$\frac{d(\rho_{21}+\rho_{12})}{dt} = -i\chi p(\rho_{21}-\rho_{12}). \quad (A5)$$

Using (A3), one may rewrite (A5) as

$$d(\rho_{21}+\rho_{12})/dt = (\chi/2V)p\frac{dp}{dt} = (\chi/4V)\frac{dp^2}{dt}. \quad (A6)$$

The formal solution of (A6), when substituted in (A4), yields

$$d(\rho_{21}-\rho_{12})/dt = -ip\{2V+\chi[(\rho_{21}+\rho_{12})_0 + (\chi/4V)(p^2-p_0^2)]\}. \quad (A7)$$

The cubic nonlinearity, i.e., the p^3 term, is already evident in (A7). When (A7) is substituted in (A3), one gets

$$\frac{dp}{dt} = -i2V(\rho_{21}-\rho_{12})_0 + \int_0^t ds[Ap(s)-Bp^3(s)], \quad (A8)$$

$$A=(\chi^2/2)p_0^2-4V^2-2V\chi(\rho_{21}+\rho_{12})_0; \quad B=(\chi^2/2). \quad (2.2)$$

The differentiation of (A8) finally leads to

$$\frac{d^2p}{dt^2} = Ap - Bp^3. \quad (2.1)$$

2. Evaluation of the arbitrary constants in the general solution (2.3)

The solution of the nonlinear equation (2.1) has been written down in Sec. II as

$$p(t) = C\,\mathrm{cn}[(C\chi/2k)(t-t_0)\,|\,k] = C\,\mathrm{dn}[(C\chi/2)(t-t_0)\,|\,1/k]. \quad (2.3)$$

In order to evaluate the arbitrary constant C in terms of p_0, $(dp/dt)_0$, and k [or $(\rho_{21}+\rho_{12})_0$], one differentiates (2.3) and uses the standard identities

$$\mathrm{sn}^2+\mathrm{cn}^2=1, \quad \mathrm{dn}^2+k^2\mathrm{cn}^2=1-k^2, \quad (A9)$$

where k is the elliptic parameter (modulus) of each of the three elliptic functions, to obtain

$$(dp/dt)_0^2 = (\chi/2k)^2(C^2-p_0^2)[C^2(1-k^2)+k^2p_0^2]. \quad (A10)$$

Defining ζ through

$$\zeta^2 = \tfrac{1}{2}[(4V/\chi)^2+(8V/\chi)(\rho_{21}+\rho_{12})_0] \quad (A11)$$

and rewriting (2.4) as

$$1/k^2 = 2[1+(1/C^2)(\zeta^2-p_0^2)], \quad (A12)$$

one eliminates k between (A10) and (A12). The final expressions for C and k are

$$C^2 = p_0^2-\zeta^2+\left[\zeta^4+(2/\chi)^2\left[\frac{dp}{dt}\right]_0^2\right]^{1/2}, \quad (A13)$$

$$k^2 = \frac{1}{2}\left\{1+(p_0^2-\zeta^2)\left[\zeta^4+(2/\chi)^2\left[\frac{dp}{dt}\right]_0^2\right]^{-1/2}\right\}. \quad (A14)$$

For the initially localized condition used in Sec. II, $(dp/dt)_0$ equals zero. Equations (A13) and (A14) show that, for that condition, $C=p_0=1$ and $k=(4V/\chi)$. The other arbitrary constant, viz., t_0 is obtained readily by putting $t=0$ in (2.3) and inverting the cn function. With the standard definition $F(\phi,k)=\int_0^\phi d\phi'(1-k^2\sin^2\phi')^{-1/2}$ of the normal elliptic integral of the first kind, t_0 is evaluated by substituting the explicit expressions for C and k in

$$t_0 = (2k/C\chi)F(\cos^{-1}(p_0/C),k). \quad (A15)$$

[1]A. C. Scott, F. Y. Chu, and D. W. McLaughlin, Proc. I.E.E.E. **61**, 1443 (1973).
[2]A. S. Davydov, J. Theor. Biol. **38**, 559 (1973); Usp. Fiz. Nauk. **138**, 603 (1982) [Sov. Phys. Usp. **25**, 898 (1982)], and references therein.
[3]D. K. Campbell, A. R. Bishop, and K. Fesser, Phys. Rev. B **26**, 6862 (1982).
[4]*Hydrogen in Metals,* edited by G. Alefeld and J. Völkl (Springer, New York, 1978), Vol. 1.
[5]T. D. Holstein, Ann. Phys. **8**, 325 (1959); **8**, 343 (1959).
[6]D. Emin, Phys. Today **35**(6), 34 (1982) and references therein.
[7]Y. Toyozawa, in *Organic Molecular Aggregates,* edited by P. Reineker, H. Haken, and H. C. Wolf (Springer-Verlag, Berlin, 1983), and references therein.
[8]J. C. Eilbeck, A. C. Scott, and P. S. Lomdahl, Chem. Phys. Lett. **113**, 29 (1985); Physica **16D**, 318 (1985).
[9]S. Takeno, Prog. Theor. Phys. **73**, 853 (1985).
[10]D. W. Brown, K. Lindenberg, and B. J. West, Phys. Rev. A **33**, 4104 (1986); **33**, 4110 (1986); J. Chem. Phys. **84**, 1574 (1986).
[11]P. S. Lomdahl and W. C. Kerr, in Physics of Many Particle Systems, edited by S. Davydov (unpublished).
[12]V. M. Kenkre and D. K. Campbell, Phys. Rev. B **34**, 4959 (1986).
[13]T. Springer, in *Quasielastic Neutron Scattering for the Investigation of Diffusive Motions in Solids and Liquids,* edited by G. Höhler (Springer, Berlin, 1972).
[14]H. Wipf, A. Magerl, S. M. Shapiro, S. K. Satija, and W. Thomlinson, Phys. Rev. Lett. **46**, 947 (1981).
[15]A. Magerl, A. J. Dianoux, H. Wipf, K. Neumaier, and I. S. Anderson, Phys. Rev. Lett. **56**, 159 (1986).
[16]V. M. Kenkre and D. W. Brown, Phys. Rev. B **31**, 2479 (1985).
[17]D. W. Brown and V. M. Kenkre, J. Phys. Chem. Solids **46**, 579 (1985); **47**, 289 (1986).
[18]L. Van Hove, Phys. Rev. **95**, 249 (1954).
[19]S. W. Lovesay, *Condensed Matter Physics: Dynamic Correlations* (Benjamin, Reading, 1980).
[20]H. Scher and M. Lax, Phys. Rev. B **7**, 4491 (1973).
[21]V. M. Kenkre, R. Kühne, and P. Reineker, Z. Phys. B **41**, 177 (1981).
[22]K. W. Kehr in *Hydrogen in Metals,* Ref. 4; K. W. Kehr and D. Richter, Solid State Commun. **20**, 477 (1976); J. W. Haus and K. W. Kehr, J. Phys. Chem. Solids **40**, 1019 (1979).
[23]We use the symbol q here to denote a *dimensionless* wave vector rather than a quantity with the dimensions of an inverse length.
[24]D. W. Brown and V. M. Kenkre, J. Phys. Chem. Solids (to be published).
[25]Paul F. Byrd and Morris D. Friedman, *Handbook of Elliptic Integrals for Engineers and Scientists,* 2nd ed. (Springer, New York, 1971).
[26]See, e.g., *Handbook of Mathematical Functions,* edited by M. Abramovitz and A. Stegun (Dover, New York, 1972).
[27]P. Reineker, in *Exciton Dynamics in Molecular Crystals and Aggregates,* edited by G. Höhler (Springer, Berlin, 1982).
[28]R. J. Silbey, Ann. Rev. Phys. Chem. **27**, 203 (1976).
[29]V. M. Kenkre, in *Exciton Dynamics in Molecular Crystals and Aggregates,* edited by G. Höhler (Springer, Berlin, 1982).
[30]V. M. Kenkre, Phys. Rev. B **12**, 2150 (1975).
[31]A. H. Zewail and C. B. Harris, Phys. Rev. B **11**, 935 (1975); **11**, 952 (1975).
[32]S. Stryer and R. P. Haugland, Proc. Nat. Acad. Sci. USA **58**, 719 (1967).
[33]T. S. Rahman, R. S. Knox, and V. M. Kenkre, Chem. Phys. **44**, 197 (1979).
[34]See, e.g., A. Maradudin, in *Solid State Physics,* edited by F. Seitz and D. Turnbull (Academic, New York, 1966), Vol. 18; M. Lax, J. Chem. Phys. **20**, 1752 (1952).
[35]M. Schwörer and H. C. Wolf, Proc. Colloq. AMPERE **14**, 544 (1966); Mol. Cryst. **3**, 177 (1967).
[36]R. Kopelman, in *Radiationless Processes in Molecules and Condensed O Phases,* edited by F. K. Fong (Springer, Berlin, 1976).
[37]D. Burland and A. Zewail, Adv. Chem. Phys. **50**, 385 (1980).
[38]R. S. Knox, in *Tunneling in Biological Systems,* edited by Britton Chance (Academic, New York, 1979); in *Primary Processes in Photosynthesis,* edited by J. Barber (North-Holland, Amsterdam, 1977).
[39]H. Haken and P. Reineker, Z. Phys. **249**, 253 (1972); P. Reineker, Z. Naturforsch. **29a**, 282 (1974).
[40]S. Rackovsky and R. Silbey, Mol. Phys. **25**, 61 (1973).
[41]C. Aslangul and Ph. Kottis, Phys. Rev. B **10**, 4364 (1974).
[42]J. A. Krumhansl and J. R. Schrieffer, Phys. Rev. B **11**, 3535 (1975).
[43]J. F. Currie, J. A. Krumhansl, A. R. Bishop, and S. E. Trullinger, Phys. Rev. B **22**, 477 (1980).